Density functional study of $Ag_{n-1}Y$ ($n = 2$–10) clusters*

Liu Xiao-Yong(刘小勇)[a], Zhu Zheng-He(朱正和)[b], and Sheng Yong(盛 勇)[a]†

[a] *College of Material Science and Engineering, Sichuan University, Chengdu* 610065, *China*
[b] *Institute of Atomic and Molecular Physics, Sichuan University, Chengdu* 610065, *China*

(Received 25 June 2010; revised manuscript received 25 May 2011)

Employing the density functional theory, we investigate the lowest-energy geometric, the stable and the electronic properties of $Ag_{n-1}Y$ ($n = 2$–10) clusters in this paper. The structural optimization and the frequency analysis are performed at the B3LYP/LANL2DZ level. Meanwhile, the differences in geometry, stability and electronic properties between Ag_n and $Ag_{n-1}Y$ ($n = 2$–10) clusters are also studied. The results show that for the doping of the yttrium atoms, the structures and the average binding lengths of the Ag_n clusters are greatly changed. In addition, the thermodynamic stabilities of the Ag_n clusters are enhanced generally with the doping of the Y atoms. In addition, the chemical stabilities of the $Ag_{n-1}Y$ clusters are still improved compared with that of the three-dimensional Ag_n clusters.

Keywords: clusters, $Ag_{n-1}Y$, stability, electronic properties

PACS: 31.15.A–, 36.40.Mr, 71.15.Mb **DOI:** 10.1088/1674-1056/20/11/113101

1. Introduction

In the last three decades, clusters have received much attention for their unique optical and magnetic properties and high catalytic activities.[1–5] As a specific example, small silver clusters are widely used in photographic material[6,7] and zeolite.[8,9] Owing to the special physical and chemical characteristics of the silver atom, the materials reveal many specific optical, redox and catalytic properties.[10]

For the silver clusters, though the d orbitals are completely filled, their close energy proximity and spatial overlap with the sp states have important effects on their structural, electronic and optical properties.[11,12] Meanwhile, these features may be enhanced, modified, or suppressed in the case of bimetallic silver clusters because of the inter-metallic interactions arising from their constitutional and morphological combinations.[13] In addition, the investigations of bimetallic silver clusters can also give us a more detail understanding of pure silver clusters. So it is interesting and important to study the bimetallic silver clusters.

Since the seminal work by Rafael *et al.*,[14] many experimental and theoretical investigations have been conducted. Bauschlicher *et al.*[15] investigated the neutral and the negatively charged clusters containing Cu, Ag and Au atoms. Willey *et al.*[16] studied the photochemistry properties of ion-molecule complexes containing silver clusters. Suzuki and Tanaka[17] investigated the electronic structures of Ge–Ag alloy clusters with the DV-Xα method. Negishi *et al.*[18] and Mitrić *et al.*[19] investigated the photoelectron spectra of gold–silver binary clusters experimentally and theoretically, respectively. Subsequently, Bonačić–Koutecký *et al.*[20] determined the structures, the ionization potentials and the vertical detachment energies for neutral and charged bimetallic Ag_mAu_n ($3 \leq (m+n) \leq 5$) by using the gradient corrected density functional method. They found that Ag atoms preferred to form more bonds than Au atoms as in the cases of pure Ag and pure Au clusters. Rossi *et al.*[21] performed the global optimizations for Ag–Ni and Ag–Cu clusters of selected sizes in a range of 30–40 atoms. At silver-rich compositions, they found a family of very stable magic structures, which were characterized as core-shell polyicosahedra and were remarkably stable. Rapallo *et al.*[22] optimized the potential energy of a wide range of binary metallic nanoclusters (Ag–Cu, Ag–Ni, Ag–Pd and Ag–Au) by using the genetic algorithm approach. They singled out the driving forces that made different structural motifs the most favourable ones for different sizes and chemical compositions. Meanwhile, Rossi *et al.*[23] performed the optimizations of Ag–Pd and Ag–Au clusters, and found that all those systems could be characterized by a small size mismatch and a weak

*Project supported by the National Natural Science Foundation of China (Grant No. 10676022).
†Corresponding author. E-mail: shengyong69@163.com
© 2011 Chinese Physical Society and IOP Publishing Ltd

tendency of the larger atoms to segregate in the surface of the smaller ones. Very recently, Yamamoto *et al.*[24] made a chemical state analysis of the silver species in Ag^+ exchanged zeolite A and Y catalysts by means of X-ray absorption fine structure (XAFS) and ultraviolet-visible (UV-Vis) spectroscopies. Harb *et al.*[25] studied the structural, the electronic and the optical properties of bimetallic Ag_nNi_n ($n \leq 7$) clusters with the density functional theory and found that the Ni atoms were surrounded by the Ag atoms. Nigam and Majumder[26] investigated the interaction of M atoms (M = Cu, Ag and Au) with small Ag_n clusters (n = 3, 6) and found that the chemical bonding natures in the cluster and slab models were similar to each other. In addition, Xiao[27] investigated the melting of icosahedral Ag–Pd bimetallic clusters by using the molecular dynamics method and found that the Ag–Pd cluster showed an irregular phenomenon before melting.

Despite the experimental and the theoretical work that has been done, there are still few investigations on sliver–yttrium clusters to our knowledge. Due to the uncompleted filled d orbitals of the Y atom, the bimetallic sliver–yttrium clusters may display some interesting physical and chemical properties. In this paper, using the density functional theory (DFT) with the relativistic effective core potential LANL2DZ basis set, we systematically investigate the geometric structures, the stabilities and the electronic properties of the $Ag_{n-1}Y$ (n = 2–10) clusters. Meanwhile, a comparison between the Ag_n and the $Ag_{n-1}Y$ (n = 2–10) clusters is also made, from which the effects of the Y atoms doped in the Ag_n (n = 2–10) clusters are obtained.

2. Computational method

The geometry optimizations and the energy calculations of the $Ag_{n-1}Y$ (n = 2–10) clusters are carried out by using the density functional theory (DFT) with the unrestricted B3LYP exchange correlation function and the relativistic effective core potential LANL2DZ basis set. All the computational work is completed with the Gaussian 03 program package.[28] To search for the lowest energy structures of the $Ag_{n-1}Y$ (n = 2–10) clusters, lots of possible initial configurations, which have different bond lengths, point groups and spin multiplicities, are used for geometry optimizations. Furthermore, the previous studies on the Ag_n clusters are also employed as a guide.[29,30] Each geometry optimization is followed by a harmonic vibrational frequency calculation to confirm that the optimized geometry corresponds to a local minimum. The convergence criteria of energy, force and displacement in all calculations are 1×10^{-6} a.u. (arbitrary units), $1\times10^{-4}/a_0$ a.u. and $1\times10^{-3}a_0$, respectively, where a_0 is the Bohr radius.

The accuracy of the current computational scheme is checked by benchmark calculations on silver and yttrium atoms. The ionization potentials of silver and yttrium atoms obtained from our calculation are 7.75 eV and 7.11 eV, respectively, which are in good agreement with the experimental data of 7.57 eV and 6.5 eV.[31] In addition, the bond length of Ag_2 (0.26 nm) is also close to the experimental result of 0.25 nm.[32] Thus, we believe that the effective core potential and the numerical basis set used in current DFT package are reasonably good to describe the $Ag_{n-1}Y$ and the Ag_n clusters.

3. Results and discussion

3.1. Equilibrium geometry

In order to discuss the effects of the doped yttrium atom on the silver clusters, we perform some calculations on the pure silver clusters. The lowest-energy geometric structures of the Ag_n and the $Ag_{n-1}Y$ (n = 2–10) clusters as well as their isomer structures are shown in Fig. 1, where the impurity atoms are indicated by dark spheres. Panel (a) shows the lowest-energy structure and panels (b), (c) and (d) show the isomer structures.

According to Fig. 1, the lowest-energy structures of AgY and Ag_2Y are similar to those of Ag_2 and Ag_3. However, when the number of the atoms is in the range from 4 to 10, obvious differences between the $Ag_{n-1}Y$ and the Ag_n clusters appear. In the case of four atoms, the lowest-energy structure of Ag_3Y is a triangle with the Y atom in the centre, while the corresponding structure of Ag_4 is a planate diamond. For Ag_4Y and Ag_5Y, the lowest-energy structures have become three-dimensional (3D), while those of Ag_5 and Ag_6 are still two-dimensional (2D). When the atom number increases to 7, the Ag_7 clusters have a 3D pentagonal bipyramid structure and the geometry of the lowest-energy Ag_6Y still shows great difference from that of Ag_7. When the number of the atoms is in the range from 8 to 10, the geometric configurations of the silver clusters can be viewed as a structure based on the Ag_8 cluster, while the $Ag_{n-1}Y$ clusters do not display such a growth pattern, indicating that the doped

Y atom breaks the growth pattern of the silver cluster.

From the above results, we can discover that the geometries of $Ag_{n-1}Y$ tend to be three-dimensional compared with those of the pure silver clusters. The reason is that in the effective core potential, the valence shell of the Y atom is $4d^15s^2$, the d orbitals are not completely filled. Thus, there are more sites for the Y atom to be bound with other atoms. The $Ag_{n-1}Y$ clusters prefer to form a three-dimensional structure, which is more stable.

In addition, comparing the lowest-energy structures with the corresponding isomers of the $Ag_{n-1}Y$ (n = 4–10) clusters, we find that the Y atoms are inclined to bind more Ag atoms in the lowest-energy geometries, indicating that the more Ag–Y bonds the cluster has, the more stable the structure is. As the Y atom is larger than the Ag atom, it is difficult for the Y atom to be in the centre of the Ag atoms.

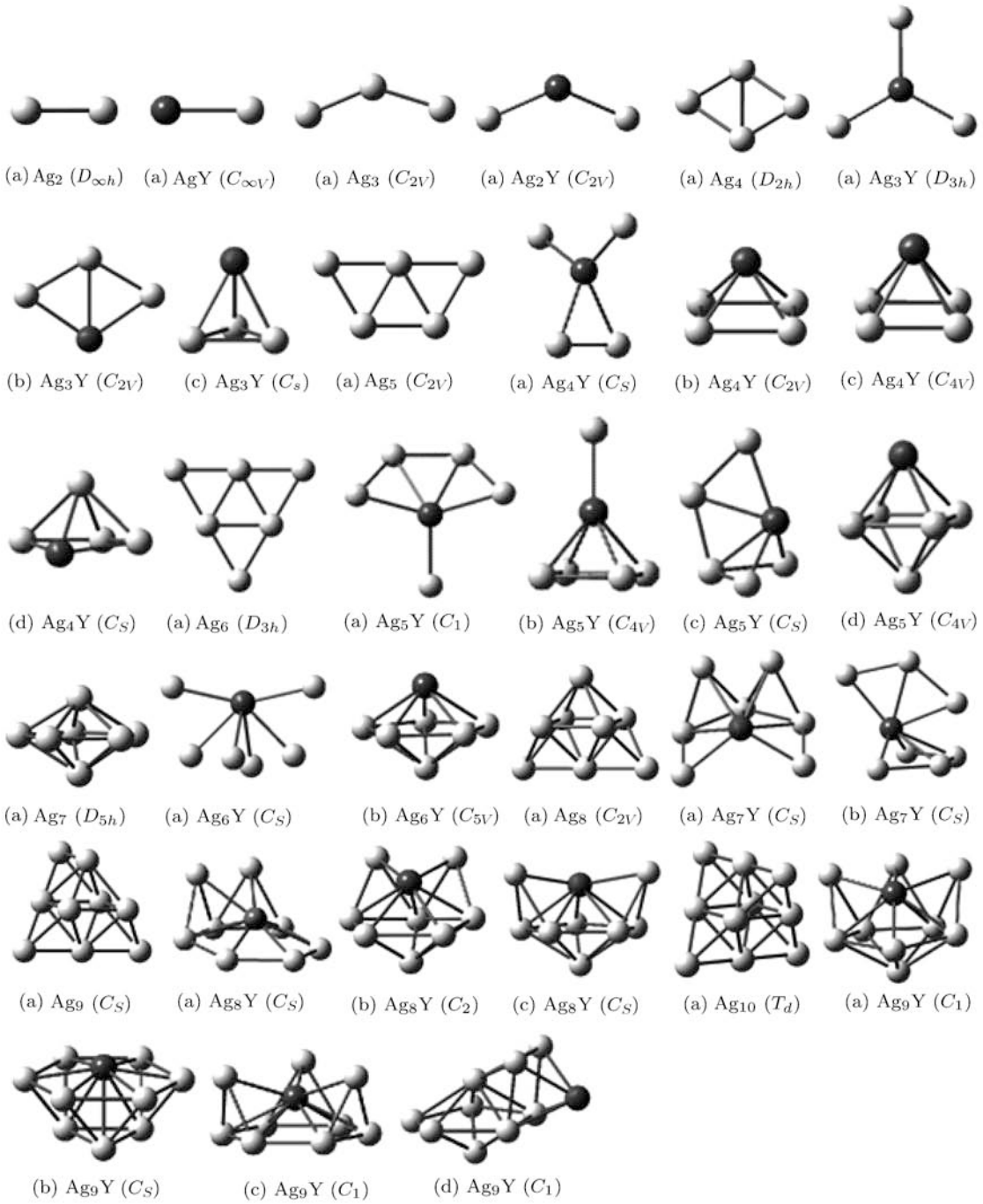


Fig. 1. (a) The lowest-energy geometric structures of Ag_n and $Ag_{n-1}Y$ (n = 2–10) clusters and (b)–(d) the corresponding isomer structures.

Figure 2 and Table 1 shows the average bond lengths of the $Ag_{n-1}Y$ and the Ag_n ($n = 2$–10) clusters in the lowest-energy state. The R represents the average bond length of a cluster and is given by $R = 1/N_b \sum R_{ij}$, where R_{ij} represents the nearest distance between atoms i and j, N_b refers to the number of the atoms with interdistance $R_{ij} \leq 0.34$ nm. Obviously, we can find that the average bond length of $Ag_{n-1}Y$ is longer than that of Ag_n. The reason is that the radius of the Y atom is larger than that of the Ag atom. Meanwhile, we also discover that there are leaps between the 3D and the 2D structures for the two kinds of clusters, which may be a result of the mutations of the cluster geometry.

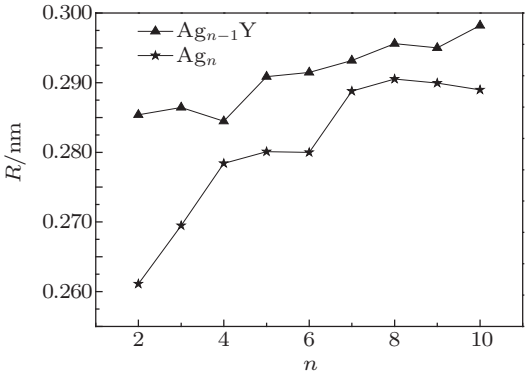


Fig. 2. Average bond lengths versus cluster size.

Table 1. Geometric parameters of $Ag_{n-1}Y$ and Ag_n ($n = 2$–10) clusters.

Clusters	Multiplicity	Symmetry	R/nm	Clusters	Multiplicity	Symmetry	R/nm
Ag_1Y	1	$C_{\infty V}$	0.2854	Ag_2	1	$D_{\infty h}$	0.2611
Ag_2Y	2	C_{2V}	0.2864	Ag_3	2	C_{2V}	0.2694
Ag_3Y	1	D_{3h}	0.2845	Ag_4	1	D_{2h}	0.2784
Ag_4Y	2	C_S	0.2909	Ag_5	2	C_{2V}	0.2801
Ag_5Y	1	C_1	0.2915	Ag_6	1	D_{3h}	0.2800
Ag_6Y	2	C_S	0.2932	Ag_7	2	D_{5h}	0.2875
Ag_7Y	1	C_S	0.2956	Ag_8	1	C_{2V}	0.2905
Ag_8Y	2	C_S	0.2950	Ag_9	2	C_S	0.2889
Ag_9Y	1	C_1	0.2982	Ag_{10}	1	T_d	0.2888

3.2. Stability of clusters

The stability of the cluster structure can be checked by the average binding energy (E_b), the second difference in energy ($\Delta_2 E$) and the gaps between the highest occupied molecular orbital (HOMO) and the lowest unoccupied molecular orbital (LUMO) (E_g).

Figure 3 displays the average binding energies of the $Ag_{n-1}Y$ and the Ag_n ($n = 2$–10) clusters. The expressions for the average binding energies of $Ag_{n-1}Y$ and Ag_n can be given as

$$E_b[Ag_{n-1}Y] = ((n-1)E[Ag] + E[Y] - E[Ag_{n-1}Y])/n, \quad (1)$$

$$E_b[Ag_n] = (nE[Ag] - E[Ag_n])/n, \quad (2)$$

where $E[x]$ is the total binding energy of the x system. From Fig. 3, we find that the average binding energy of $Ag_{n-1}Y$ (except for AgY) is obviously higher than that of Ag_n, which may be caused by the electronegativity difference between Y and Ag atoms. For a more detailed understanding, more basic studies should be carried out.

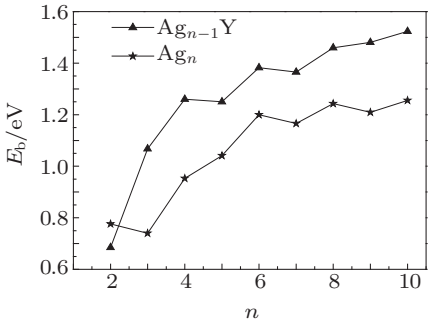


Fig. 3. Average binding energies versus cluster size.

Moreover, we also see that the average binding energies of the Ag_n and the $Ag_{n-1}Y$ ($n = 2$–10) clusters generally increase with the growing atom number, indicating that the stability increases with the growing atom number.

In Figs. 4(a) and 4(b), we plot $\Delta_2 E$ and E_g of the $Ag_{n-1}Y$ and the Ag_n ($n = 2$–10) clusters each as

a function of the cluster size. The formulas for $\Delta_2 E$ and E_g of Ag_n and $Ag_{n-1}Y$ can be given as

$$\Delta_2 E[Ag_n] = E[Ag_{n+1}] + E[Ag_{n-1}] - 2E[Ag_n], \quad (3)$$

$$\Delta_2 E[Ag_{n-1}Y] = E[Ag_{n-2}Y] + E[Ag_nY] - 2E[Ag_{n-1}Y], \quad (4)$$

$$E_g = E_{LUMO} - E_{HOMO}. \quad (5)$$

From Figs. 4(a) and 4(b), we find that both $\Delta_2 E$ and E_g of $Ag_{n-1}Y$ and Ag_n exhibit odd–even oscillations. The even-number clusters are more stable than the neighbouring odd-size ones. It indicates that the doped Y atoms do not change the odd–even oscillations of the Ag_n clusters. The odd–even oscillations can be understood based on the electron pairing effect. In our calculation, the valence shells of Y and Ag are $4d^15s^2$ and $4d^{10}5s^1$, respectively. Odd (even) size clusters each has an odd (even) total number valence electrons, and their HOMO is singly (doubly) occupied. The electron in a doubly occupied HOMO feels a stronger effective core potential, since the electron screening is weaker for electrons in the same orbital than that for the inner-shell electrons. Therefore, the binding energy of a valence electron in a cluster of even size is larger than that in an odd size one.

Meanwhile, as obviously shown in Fig.4(b) and Table 2, the HOMO–LUMO gaps of Ag_3Y and Ag_6 are larger than those of other $Ag_{n-1}Y$ and Ag_n clusters, respectively, which indicates that Ag_3Y and Ag_6 are more stable than other $Ag_{n-1}Y$ and Ag_n clusters. In addition, a comparison of E_g between $Ag_{n-1}Y$ and Ag_n obviously shows that the doped Y atoms generally reduce the E_g values of the Ag_n clusters. This can be explained by the different valence electron distributions of the Ag and the Y atoms. In our calculation, the bonding electrons of the Ag atom origin from the 5s orbital, while the bonding electrons of the Y atom are sourced from the 4d and the 5s orbitals. With the addition of the Y atom, the total number of bonding electrons of the clusters increases, which will provide more active electrons and enhance the delocalization of the HOMO and the LUMO orbitals and finally result in the decrease of E_g.

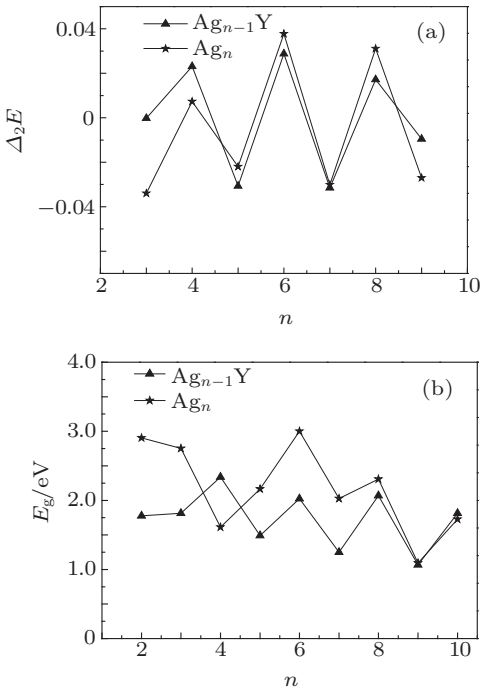


Fig. 4. (a) The second difference in energy and (b) the HOMO–LUMO gaps versus cluster size.

Table 2. The E_b, $\Delta_2 E$ and E_g of $Ag_{n-1}Y$ and Ag_n (n = 2–10) clusters.

Clusters	E_b/eV	$\Delta_2 E$/eV	E_g/eV	Clusters	E_b/eV	$\Delta_2 E$/eV	E_g/eV
Ag_1Y	0.6851	–	1.7772	Ag_2	0.7763	–	2.9054
Ag_2Y	1.0674	–0.0002	1.8142	Ag_3	0.7396	–0.0340	2.75134
Ag_3Y	1.2602	0.0231	2.3380	Ag_4	0.9528	0.0073	1.6123
Ag_4Y	1.2501	–0.0307	1.4906	Ag_5	1.0409	–0.022	2.1652
Ag_5Y	1.3825	0.0288	2.0256	Ag_6	1.1995	0.0378	3.0009
Ag_6Y	1.3651	–0.0315	1.2495	Ag_7	1.1658	–0.0301	2.0269
Ag_7Y	1.4593	0.0172	2.0692	Ag_8	1.2429	0.0311	2.3075
Ag_8Y	1.4805	–0.0096	1.0661	Ag_9	1.2089	0.0068	1.092
Ag_9Y	1.5234	–	1.8147	Ag_{10}	1.1631	–	1.7263

3.3. Electronic properties of clusters

In cluster physics, the electronic properties of clusters can be shown by the vertical ionization energy (IP) and the electron affinity energy (EA).

Figure 5 and Table 3 show the IP and the EA of the $Ag_{n-1}Y$ and the Ag_n (n = 2–10) clusters. As shown in Fig. 5(a), compared with that of the Ag_n clusters, the odd–even oscillations in the vertical ionization energy of the $Ag_{n-1}Y$ clusters become weaker

because of the d orbitals and the bonding electrons added by the Y atoms. In addition, when the atom number is in the range from 7 to 10, the IP values of the $Ag_{n-1}Y$ clusters are higher than those of the Ag_n clusters, which indicates that the Y atoms can improve the chemical stabilities of the 3D Ag_n clusters. However, the EA values of $Ag_{n-1}Y$ and Ag_n ($n = 2$–10) in Fig. 5(b) show obvious odd–even oscillations, which indicates that the effect on the variation trend of the Ag_n cluster is not great.

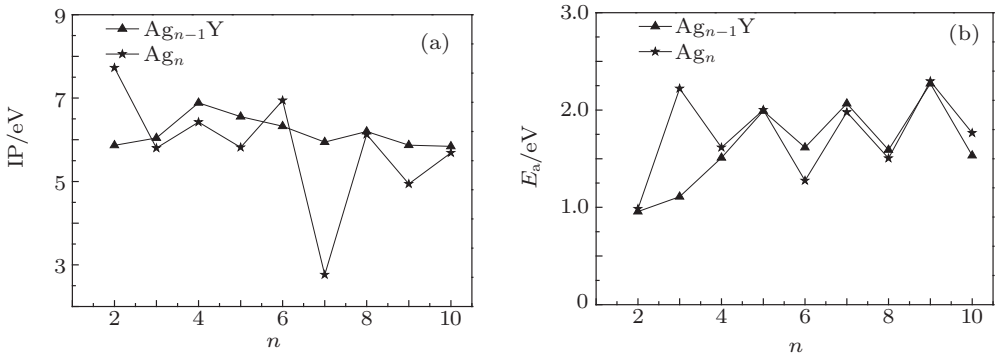


Fig. 5. (a) Vertical ionization energy and (b) electron affinity energy versus cluster size.

Table 3. IP and EA of $Ag_{n-1}Y$ ($n = 2$–10) and Ag_n clusters.

Clusters	IP/eV	EA/eV	Clusters	IP/eV	EA/eV
Ag_1Y	5.8653	0.9560	Ag_2	7.7259	0.9847
Ag_2Y	6.0416	1.1090	Ag_3	5.8006	2.2206
Ag_3Y	6.8845	1.5092	Ag_4	6.4230	1.6155
Ag_4Y	6.5564	1.9908	Ag_5	5.8168	2.0015
Ag_5Y	6.3262	1.6153	Ag_6	6.9452	1.2737
Ag_6Y	5.9448	2.0659	Ag_7	5.7605	1.978
Ag_7Y	6.19786	1.5907	Ag_8	6.1302	1.5039
Ag_8Y	5.8723	2.2713	Ag_9	4.9417	2.2963
Ag_9Y	5.84049	1.5333	Ag_{10}	5.6853	1.7645

4. Conclusion

Based on the above discussion of the Ag_n and the $Ag_{n-1}Y$ ($n = 2$–10) clusters in the aspects of geometric, stable and electronic properties, the main conclusions can be made as follows. (i) The lowest-energy structures of the $Ag_{n-1}Y$ clusters tend to be three-dimensional and the Y atoms are inclined to bind with more Ag atoms. (ii) With the addition of the Y atoms, the bond length of $Ag_{n-1}Y$ is longer than that of Ag_n. Meanwhile, there exist leaps between the 3D and 2D structures for both the $Ag_{n-1}Y$ and the Ag_n clusters. (iii) The thermodynamic stability of the Ag_n clusters generally increases with the doped Y atoms based on the average binding energy study. In addition, the odd–even oscillations in $\Delta_2 E$ and E_g of the Ag_n clusters are maintained. (iv) With the dope of the Y atoms, the odd–even oscillation in the IP value of the Ag_n cluster is weakened, while the odd–even oscillation in the EA value of the Ag_n cluster is retained.

References

[1] Valden M, Lai X and Goodman D W 1998 *Science* **281** 1647
[2] Rossi G, Rapallo A, Mottet C, Fortunelli A, Baletto F and Ferrando R 2004 *Phys. Rev. Lett.* **93** 105503
[3] Qi K T, Mao H P, Wang H Y and Sheng Y 2010 *Chin. Phys.* B **19** 033602
[4] Zhao L X, Feng X J, Cao T T, Liang X and Luo Y H 2009 *Chin. Phys.* B **18** 2709
[5] Bai Y L, Chen X R, Cheng X H and Yang X D 2007 *Chin. Phys.* **16** 0700
[6] Hailstone R K and de Keyzer R 2001 *J. Phys. Chem.* B **105** 7533
[7] Gutta P and Hoffmann R 2003 *J. Phys. Chem.* A **107** 8184
[8] Zhao S, Liu Z P, Li Z H, Wang W N and Fan K N 2006 *J. Phys. Chem.* A **110** 11537
[9] Schoonheydt R A and Leeman H 1989 *J. Phys. Chem.* **93** 2048
[10] Baba T and Inazu K 2006 *Chem. Lett.* **35** 142

[11] Idrobo J C and Öğüt S 2005 *J. Phys. Chem.* B **72** 085445
[12] Kim S H, Medeiros-Ribeiro G, Ohlberg D A A, Williams R S and Heath J R1999 *J. Phys. Chem.* B **103** 10341
[13] He J H, Ichinose I, Kunitake T, Nakao A, Shiraishi Y and Toshima N 2003 *J. Am. Chem. Soc.* **125** 11034
[14] Uson R, ForniCs J, Tomas M, Cotton F A and Falvello L R 1984 *J. Am. Chem. Soc.* **106** 2482
[15] Bauschlicher C W Jr., Langhoff S R and Partridge H 1989 *J. Chem. Phys.* **91** 2412
[16] Willey K F, Cheng P Y, Bishop M B and Ducan M A 1991 *J. Am. Chem. Soc.* **113** 4711
[17] Suzuki A and Tanaka K 1998 *Jpn. J. Appl. Phys.* **37** 4872
[18] Negishi Y, Nakajima Y and Kaya K 2001 *J. Chem. Phys.* **115** 3657
[19] Mitrić R, Hartmann M, Stanca B, Bonačić-Koutecký V and Fantucci P 2001 *J. Phys. Chem.* A **105** 8892
[20] Bonačić-Koutecký V, Burda J, Mitrić R and Ge M 2002 *J. Chem. Phys.* **117** 3120
[21] Rossi G, Rapallo A, Mottet C, Fortunelli A, Baletto F and Ferrando R 2004 *Phys. Rev. Lett.* **93** 105503
[22] Rapallo A, Rossi G, Ferrando R, Fortunelli A, Curley B C, Lloyd L D, Tarbuck G M and Johnston R L 2005 *J. Chem. Phys.* **122** 194308
[23] Rossi G, Ferrando R, Rapallo R, Curley B C, Lloyd L D and Johnston R L 2005 *J. Chem. Phys.* **122** 194309
[24] Yamamoto T, Takenaka S, Tanaka T and Baba T 2009 *14th International Conference on X-Ray Absorption Fine Structure*, July 26–31, 2009, Camerino, Italy, p. 12171
[25] Harb M, Rabilloud F and Simon D 2009 *J. Chem. Phys.* **131** 174302
[26] Nigam S and Majumder C 2010 *J. Phys.: Condens. Matter* **22** 435001
[27] Xiao X Y 2010 *Chin. Phys.* B **19** 113604
[28] Frisch M J, Trucks G W and Schlegel H B 2003 *Gaussian 03* (Revision A.7, Gaussian Inc., Pittsburgh, USA)
[29] Idrobo J C and Öğüt S 2005 *Phys. Rev.* B **72** 085445
[30] Li X B, Wang H Y, Tang Y J, Xu G L, Mao H P, Li C Y and Zhu Z H 2004 *J. At. Mol. Phys.* **21** 388(in Chinese)
[31] Kittle C 1996 *Introduction to Solid State Physics* (7th edn.) (New York: Wiley) p. 54
[32] Beutel V, Krämer H G, Bhale G L, Kuhn M, Weyers K and Demtröder W 1993 *J. Chem. Phys.* **98** 2699